Normal Mode Waves in an Elastic Plate,??

Normal Mode Waves in an Elastic Plate, II

By Kôhei Nakamura

Geophysical Institute, Faculty of Science, Tôhoku University

(Received Sept. 15, 1960)

Abstract

The structure of the dispersion curves of the normal mode waves formed by P and SV waves in an elastic homogeneous plate with the Poisson ratio 1/4, is elucidated by examining minutely the characteristic equations, and by using the dispersion curves of a hypothetical plate which transmits only a single bodily wave. In the analysis, special emphasis is laid on the behaviours of the dispersion curves at some particular incident angles of S, and those at the lattice points which are successfully used by Tolstoy and Usdin in their study of group velocity of higher modes. The frequency which makes the group velocity equal to the velocity of S, and the maximum group velocity in higher modes, together with its corresponding frequency, are obtained as functions of mode number. A remark is made on the "negative phase velocity" suggested by Tolstoy and Usdin. In the larger part of the paper, the lowest modes $\Pi_0^{\pm}$ which have the Rayleigh wave velocity at infinite frequency are exlcuded, as the behaviours of such modes are well known.

1 Introduction

Various results have been published on the propagation of elastic waves in a plate since the original contribution of Lord Rayleigh (1889) and Sir Horace Lamb (1917). A comprehensive bibliography on the subject and the allied problems in cylindrical bars is contained for example in the text book by M. Ewing *et al.* (1957).

We will summarize some important results obtained recently. It is suggested by Y. Satô (1951) that M_1 and M_2 waves in a two-layered half space bear correspondence respectively to the symmetric and anitsymmetric types of motion in a plate. A. N. Holden (1951) has given a rather complete analysis about the nature of the dispersion curves of some modes of symmetric type. R.D. Fay and O.V. Fortier (1951) have made an extensive series of measurements on the transmission of sound through a steel plate submerged in water. They have shown in their analysis that the velocity equation can be derived from a consideration of the constructive interference of body waves, which is the condition to be satisfied for the free stable waves to exist. I. Tolstoy and E. Usdin (1953), developing the method of Fay and Fortier, have examined the velocity equations for various cases of layered media based on the interference principle of wave guide propagation, without formulating the problems as boundary value problems. They also have distinguished formally the M_1 and M_2 waves, but, physical ground of the separation into M_1 and M_2 remains still obscure. R.R. Aggarwar and E.A.G. Show (1954), and R.H. Lyon (1955) have found attenuated modes of the solution. Lyon has investigated the amplitude of symmetrical vibration near a

driving area on a plate at which a periodic vertical force is applied. R.D. MINDLIN *et al.* (1951), (1956) have carried out an extensive numerical work on the vibration of a plate of finite or infinite area. TOLSTOY and USDIN (1956) have calculated the group velocities of a plate for some modes, and found a new dispersive property of a plate with the Poisson ratio 1/4, that is, the negative phase velocity. They also have shown very interesting features of dispersion curves of extremely high modes by using the lattice points introduced by MINDLIN. J.W.C. SHERWOOD (1958) has showed the existence of complex eigenvalues and laid emphasis on the eigenmotions associated with complex eigenvalues to interprete some results obtained by other writers, including the negative phase velocity of TOLSTOY and USDIN. K. TAJIME (1958) has discussed the behaviours of dispersion curves when the Posisson ratio is changed between 0 and 0.5, and obtained on the dispersion curves the parts where significant amplitudes are to be expected for a compressional cylindrical source.

We have seen in the first paper that the normal mode waves formed by SH waves in a plate are decomposed into the symmetric and antisymmetric parts. In this case, the phase change in reflection at the boundaries is always zero. Because, in the normal mode waves formed by P and SV, the two bodily waves are combined by the law of reflection at the free surfaces such that the constructive interference is realized, the main feature of the dispersion curves will be obtained by the aid of two sets of dispersion curves of hypothetical plates which transmit respectively P and S alone. The plate which supports only P is a liquid one, while the plate which transmits only S is an incompressible soild, the Poisson ratios of both plates being 0.5. In these plates, the vertical or horizontal displacement remains unchanged in reflection at the free boundaries. Each plate has both the symmetric and antisymmetric modes, and the types of modes are interchanged if the phase change is π, as in the case of a rigid boundary. It can be seen, that from the reflection law at the free boundaries, at some particular incident angles of S, the transformation of one body wave to the other is extraordinary. Examination of the characteristic equations at such incident angles of S, if combined with the conditions of constructive interference of the hypothetical plates above mentioed, will give the general features of the dispersion curves. By such an analysis, particular properties of dispersion curves will be obtained analytically, without drawing whole curves.

2 Free Wave Solution

Consider a homogeneous isotropic plate with uniform width $2H$ and infinite area. We choose the rectangular coordinates (x, y, z), so that z-axis is perpendicular to the plane surfaces of the plate, x, y-axes lie in the median plane (see Fig. 1).

Let ϑ be the displacement vector, λ and μ the Lamé's constants, and ρ the density. The equation of motion is

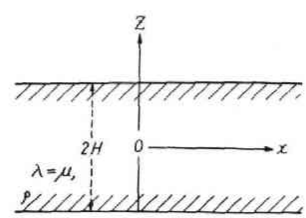

Fig. 1.

$$\rho \frac{\partial^2 \vartheta}{\partial t^2} = (\lambda+\mu)\,\mathrm{grad}\,\mathrm{div}\,\vartheta + \mu\,\mathrm{div}\,\mathrm{grad}\,\vartheta . \tag{1}$$

If we put

$$\vartheta = \mathrm{grad}\,\varphi + \mathrm{rot}\,a , \tag{2}$$

where a has the componetns $(0, \psi, 0)$, then ϑ becomes a solution of (1), provided that φ and ψ respectively satisfy the equations

$$\nabla^2 \varphi = \frac{1}{v_p^2}\frac{\partial^2 \varphi}{\partial t^2} , \quad \nabla^2 \psi = \frac{1}{v_s^2}\frac{\partial^2 \psi}{\partial t^2} , \tag{3}$$

where $v_p = \sqrt{(\lambda+2\mu)/\rho}$ and $v_s = \sqrt{\mu/\rho}$ are velocities the of P and S waves.

If a simple harmonic motion with the time factor $e^{i\omega t}$ is assumed, (3) becomes

$$(\nabla^2 + h^2)\,\varphi = 0 , \quad (\nabla^2 + k^2)\,\psi = 0 , \tag{4}$$

where

$$h = \frac{\omega}{v_p} \quad \text{and} \quad k = \frac{\omega}{v_s} . \tag{5}$$

The components of displacement are written

$$u = \frac{\partial \varphi}{\partial x} - \frac{\partial \psi}{\partial z} , \quad v = 0 , \quad w = \frac{\partial \varphi}{\partial z} + \frac{\partial \psi}{\partial x} , \tag{6}$$

and the components of stress are given by

$$P_{zx} = \mu\left(\frac{\partial u}{\partial z} + \frac{\partial w}{\partial x}\right), \quad P_{zy} = \mu\left(\frac{\partial w}{\partial y} + \frac{\partial v}{\partial z}\right), \quad P_{zz} = \lambda\,\mathrm{div}\,\vartheta + 2\mu\frac{\partial w}{\partial z} . \tag{7}$$

Consider a set of potentials in the form of plane waves propagated in the xz-plane,

$$\left.\begin{aligned} \varphi &= \left[A e^{-ikzM} + B e^{ikzM}\right] e^{-ikx\sin w} , \\ \psi &= \left[C e^{-ikzN} + D e^{ikzN}\right] e^{-ikx\sin w} , \end{aligned}\right\} \tag{8}$$

where w represents, if it is real, the angle made by the z-axis and the wave-normal of SV waves, and

$$m = \frac{v_p}{v_s} , \quad M = \sqrt{\frac{1}{m^2} - \sin^2 w} , \quad N = \cos w . \tag{9}$$

The time factor $e^{i\omega t}$ will be suppressed hereafter.

Since the general motion of an infinite plate consists of two independent modes of motion, symmetric and antisymmetric with respect to the median plane, it is convenient to decompose the set of potentials (8) into two parts.

The symmetric motion is represented by

$$\left.\begin{aligned} \varphi_s &= E_s \cos\alpha'\, e^{-ikx\sin w} , \\ \psi_s &= i F_s \sin\beta'\, e^{-ikx\sin w} , \end{aligned}\right\} \tag{10}$$

and the antisymmetric motion, by

$$\left.\begin{aligned} \varphi_a &= i E_a \sin\alpha'\, e^{-ikx\sin w} , \\ \psi_a &= F_a \cos\beta'\, e^{-ikx\sin w} , \end{aligned}\right\} \tag{11}$$

where
$$E_s = B+A, \quad E_a = B+A, \quad F_s = D-C, \quad F_a = D+C,$$
$$\alpha' = k z M, \quad \beta' = k z N. \tag{12}$$

Hereafter in this section, the two types of motion will be discussed separately.

(a) Symmetric motion.

Substituting (10) into the expressions of P_{zx} and P_{zz} in (7) yields

$$\left.\begin{aligned} P_{zx} &= i\mu k^2 \left[2 \sin wM \sin \alpha' E_s + b \sin \beta' F_s\right] e^{-ikx \sin w}, \\ P_{zz} &= \mu k^2 \left[-b \cos \alpha' E_s + 2 \sin w N \cos \beta' F_s\right] e^{-ikx \sin w}, \end{aligned}\right\} \tag{13}$$

where
$$b = 1 - 2\sin^2 w. \tag{14}$$

The boundary conditions are that the boundary surfaces are free from stress. Two conditions that $P_{zx}=0$, at $z=\pm H$ can be written from (13) in an identical form
$$(2 \sin wM \sin \alpha) E_s + (b \sin \beta) F_s = 0, \tag{15}$$
and the other two conditions that $P_{zz}=0$ at $z=\pm H$ also become an identical form
$$(-b \cos \alpha) E_s + (2 \sin w N \cos \beta) F_s = 0, \tag{16}$$
where
$$\alpha = kHM, \qquad \beta = kHN. \tag{17}$$
Elimination of E_s and F_s from (15) and (16) gives a characteristic equation
$$Z_s = G \tan \alpha + K \tan \beta = 0, \tag{18}$$
where
$$G = 4 \sin^2 w M N, \qquad K = b^2 = (1-2\sin^2 w)^2. \tag{19}$$

The components of displacement are obtained from (6), (10), (15) and (18)

$$\left.\begin{aligned} u &= -ik \sin w \cos \alpha E_s A_s^*, \\ w &= -kM \cos \alpha E_s B_s^*, \end{aligned}\right\} \tag{20}$$

where

$$\left.\begin{aligned} A_s^* &= \left[\frac{\cos \alpha'}{\cos \alpha} + \frac{b}{2\sin^2 w} \frac{\cos \beta'}{\cos \beta}\right], \\ B_s^* &= \left[\frac{\sin \alpha'}{\cos \alpha} - \frac{b}{2MN} \frac{\sin \beta'}{\cos \beta}\right]. \end{aligned}\right\} \tag{21}$$

(b) Antisymmetric motion

The components of stress are obtained from (7) and (11)

$$\left.\begin{aligned} P_{zx} &= \mu k^2 \left[2 \sin wM \cos \alpha' E_a + b \cos \beta' F_a\right] e^{-ikx \sin w} \\ P_{zz} &= i\mu k^2 \left[-b \sin \alpha' E_a + 2 \sin^2 w N \sin \beta' F_a\right] e^{-ikx \sin w} \end{aligned}\right\} \tag{22}$$

Two pairs of boundary conditions $P_{zx}=0$ at $z=\pm H$, and $P_{zz}=0$ at $z=\pm H$, yield respectively the equations

$$\left.\begin{aligned}(2\sin w\, M\cos\alpha)\, E_a + (b\cos\beta)\, F_a = 0\,,\\ (-b\sin\alpha)\, E_a + (2\sin w\, N\sin\beta)\, F_a = 0\,.\end{aligned}\right\} \tag{23}$$

Eliminating E_a and F_a, we have a characteristic equation

$$Z_a = G\tan\beta + K\tan\alpha = 0. \tag{24}$$

The displacements are obtained from (6) and (11)

$$\left.\begin{aligned}u_a &= k\sin w\cos\alpha\, E_a A_a{}^*\\ w_a &= i\,k\,M\cos\alpha\, E_a B_a{}^*\,,\end{aligned}\right\} \tag{25}$$

where

$$\left.\begin{aligned}A_a{}^* &= \left[\frac{\sin\alpha'}{\cos\alpha} - \frac{2MN}{b}\,\frac{\sin\beta'}{\cos\beta}\right],\\ B_a{}^* &= \left[\frac{\cos\alpha'}{\cos\alpha} + \frac{2\sin^2 w}{b}\,\frac{\cos\beta'}{\cos\beta}\right].\end{aligned}\right\} \tag{26}$$

3 Characteristic Equations and Phase Velocity

The equations (18) and (24) define respectively the symmetric and antisymmetric eigenmotions in a plate.

If we put

$$\sin w = v = \frac{v_s}{c}\,, \tag{27}$$

then, c represents the phase velocity. Putting also

$$kH = \gamma\,, \tag{28}$$

we can write (18) and (24) in terms of v and γ,

$$\left.\begin{aligned}\Gamma_s &= v^2 MN\tan\alpha + a^2\tan\beta = 0\,,\\ \Gamma_a &= v^2 MN\tan\beta + a^2\tan\alpha = 0\,,\end{aligned}\right\} \tag{29}$$

where

$$Z_s = 4\Gamma_s\,, \qquad Z_a = 4\Gamma_a\,, \qquad a = v^2 - \frac{1}{2}\,. \tag{30}$$

The dispersive property of the phase velocity will be investigated by use of the γ–v diagram. In the sequel, it will be assumed that $\lambda=\mu$ or $m=\sqrt{3}$ and hence that

$$\left.\begin{aligned}M &= \sqrt{\frac{1}{3}-v^2}\,, && v^2 < \frac{1}{3}\,,\\ &= -i\sqrt{v^2-\frac{1}{3}}\,, && v^2 > \frac{1}{3}\,,\\ N &= \sqrt{1-v^2}\,, && v^2 < 1\,,\\ &= -i\sqrt{v^2-1}\,, && v^2 > 1\,.\end{aligned}\right\} \tag{31}$$

Then, (29) can be written explicitely as follows;

$$\left\{ = v^2\sqrt{1-v^2}\sqrt{\frac{1}{3}-v^2}\,\tan\left(\gamma\sqrt{\frac{1}{3}-v^2}\right) + a^2\tan\left(\gamma\sqrt{1-v^2}\right) = 0\,, \qquad 0 < v < \frac{1}{\sqrt{3}}\,,\right.$$

$$\Gamma_s \begin{cases} = -\left[v^2\sqrt{1-v^2}\sqrt{v^2-\frac{1}{3}}\tanh\left(\gamma\sqrt{v^2-\frac{1}{3}}\right) - a^2\tan\left(\gamma\sqrt{1-v^2}\right)\right] = 0, & \frac{1}{\sqrt{3}} < v < 1, \\ = i\left[v^2\sqrt{v^2-1}\sqrt{v^2-\frac{1}{3}}\tanh\left(\gamma\sqrt{v^2-\frac{1}{3}}\right) - a^2\tanh\left(\gamma\sqrt{v^2-1}\right)\right] = 0, & 1 < v, \end{cases} \tag{32}$$

$$\Gamma_a \begin{cases} = v^2\sqrt{1-v^2}\sqrt{\frac{1}{3}-v^2}\tan\left(\gamma\sqrt{1-v^2}\right) + a^2\tan\left(\gamma\sqrt{\frac{1}{3}-v^3}\right) = 0, & 0 < v < \frac{1}{\sqrt{3}}, \\ = -i\left[v^2\sqrt{1-v^2}\sqrt{v^2-\frac{1}{3}}\tan\left(\gamma\sqrt{1-v^2}\right) + a^2\tanh\left(\gamma\sqrt{v^2-\frac{1}{3}}\right)\right] = 0, & \frac{1}{\sqrt{3}} < v < 1, \\ = i\left[v^2\sqrt{v^2-1}\sqrt{v^2-\frac{1}{3}}\tanh\left(\gamma\sqrt{v^2-1}\right) - a^2\tanh\left(\gamma\sqrt{v^2-\frac{1}{3}}\right)\right] = 0, & 1 < v. \end{cases} \tag{33}$$

From (29), we obtain the relations,

$$\left.\begin{aligned} \frac{\partial\Gamma_s}{\partial v} &= \frac{-v}{12a^2MN}\left[3a^2\alpha + 4a(2v^4-4v^2+1)\tan\alpha - \alpha v^2(8v^2-3)N^2\tan^2\alpha\right], \\ \frac{\partial\Gamma_s}{\partial\gamma} &= \frac{-N}{12a^2}\left[a^2(8v^2-3) - 3v^2M^2\tan^2\alpha\right], \\ \frac{\partial\Gamma_a}{\partial v} &= \frac{1}{12vM^2N^2}\left[\alpha v^2(8v^2-3)N^2 + 4a(2v^4-4v^2+1)\tan\alpha - 3\alpha a^2\tan^2\alpha\right], \\ \frac{\partial\Gamma_a}{\partial\gamma} &= \frac{-1}{12v^2M}\left[-3v^2M^2 + a^2(8v^2-3)\tan^2\alpha\right]. \end{aligned}\right\} \tag{34}$$

We also have

$$\frac{dv}{d\gamma_{s,a}} = -\left(\frac{\partial\Gamma_{s,a}}{\partial\gamma}\right)\Big/\left(\frac{\partial\Gamma_{s,a}}{\partial v}\right). \tag{35}$$

In calculating (34), we note that, using (29), the factor $\tan\beta$ can be expressed by the terms containing $\tan\alpha$.

4 Basic Notion about Dispersion in a Plate

Since the dispersion curves in two plates which transmit respectively only P and only S, and the reflection law of the actual plate at free boundaries are considered to be the basic matters for the analysis of the characteristic equations, a brief account on these subjects will be given.

(1) Reflection at free boundary.

The reflection coefficients at a free surface of vertical dsiplacement in P–P and P–S reflections, and those of horizontal displacement in S–P and S–S reflections are shown in Fig. 2. The phase lag in total reflection S–S is shown in Fig. 3. In these figures, w_p is the incident angle of P, and is related to w by the SNELL's law $\sin w_p = \sqrt{3}\sin w$.

It is seen from these figures that P can exist without changing into S only at A ($v=0$) and $D(v=1/\sqrt{3})$, and S can exist without being transformed to P at A, and between D and F ($v=1$). At B ($v=1/2$), P and S are completely transformed to S and P respectively. We also see that the phase change δ_v of vertical displacement

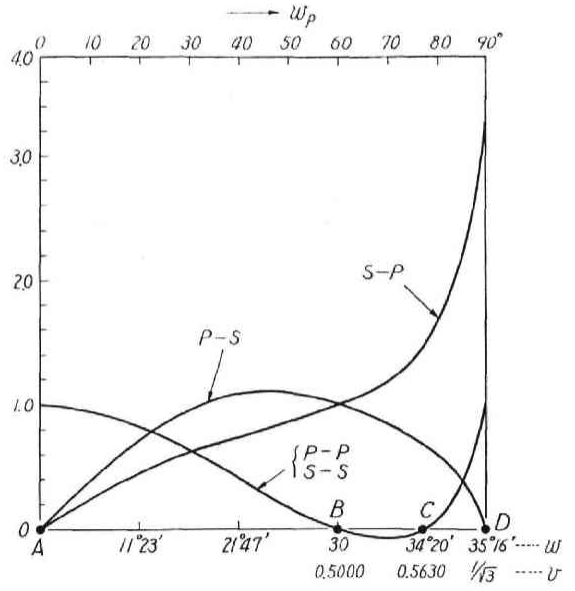

Fig. 2. Coefficients of vertical displacement in P-P and P-S reflections and those of horizontal displacement in S-S and S-P reflections. w_p: incident angle of P, w: incident angle of S, $v = \sin w$.

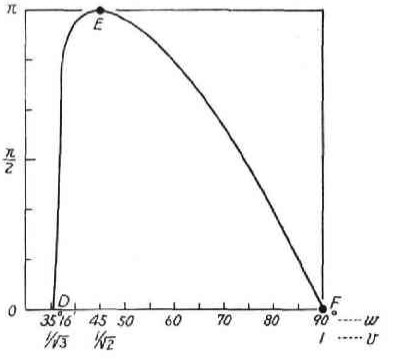

Fig. 3. Phase lag in S-S total reflection.

at A in P–P reflection is zero, and the phase change δ_h of horizontal displacement in S–S reflection is zero at A, D and F, and π at E. It should be noticed that S wave at E can be transmitted without changing into P.

(2) Dispersion curves in a plate which transmits only single body wave.

The characteristic equation of a liquid plate ($\lambda = \lambda$, $\mu = 0$), can be easily obtained. The dispersion curves P_l of the symmetric modes for the case $\delta_v = 0$ (free foundary) and those of the antisymmetirc modes for the case $\delta_v = \pi$ (rigid boundary) are identically written as

$$P_l: \ \cos a = 0 \quad \text{or} \quad \gamma\sqrt{\frac{1}{3} - v^2} = \frac{l}{2}\pi . \quad (l: \text{ odd integer}) \qquad (36)$$

The dispersion curves of the antisymmetric and symmetric modes respectively for the cases $\delta_v = 0$ and $\delta_v = \pi$ are also written in the same form;

$$P_l: \ \sin a = 0 \quad \text{or} \quad \gamma\sqrt{\frac{1}{3} - v^2} = \frac{l}{2}\pi . \quad (l: \text{ even integer}) \qquad (37)$$

In the case of a hypothetical plate ($\lambda = \infty$, $\mu = \mu$) which tansmits only S, the dispersion curves S_m of the symmetric modes for the case $\delta_h = 0$ (free boundary), and the antisymmetric modes for the case $\delta_h = \pi$ (rigid boundary) are written as

$$S_m: \ \sin \beta = 0 \quad \text{or} \quad \gamma\sqrt{1 - v^2} = \frac{m}{2}\pi . \quad (m: \text{ even}) \qquad (38)$$

and the dispersion curves of the antisymmetric and symmetric modes respectively for the cases $\delta_h=0$ and $\delta_h=\pi$ become

$$S_m:\ \cos\beta=0 \quad \text{or} \quad \gamma\sqrt{1-v^2}=\frac{m}{2}\pi\,. \quad (m:\ \text{odd})\,. \tag{39}$$

(38) and (39) have been studied in the SH-formed normal mode waves treated in the first paper. TOLSTOY and USDIN (1956), and TAJIME (1958) have used some of those curves in their analyses. It is to be noticed that, the symmetric and antisymmetric modes in each hypothetical plate are interchanged. In Fig. 4 are shown S_m and P_l respectively by dotted and broken curves.

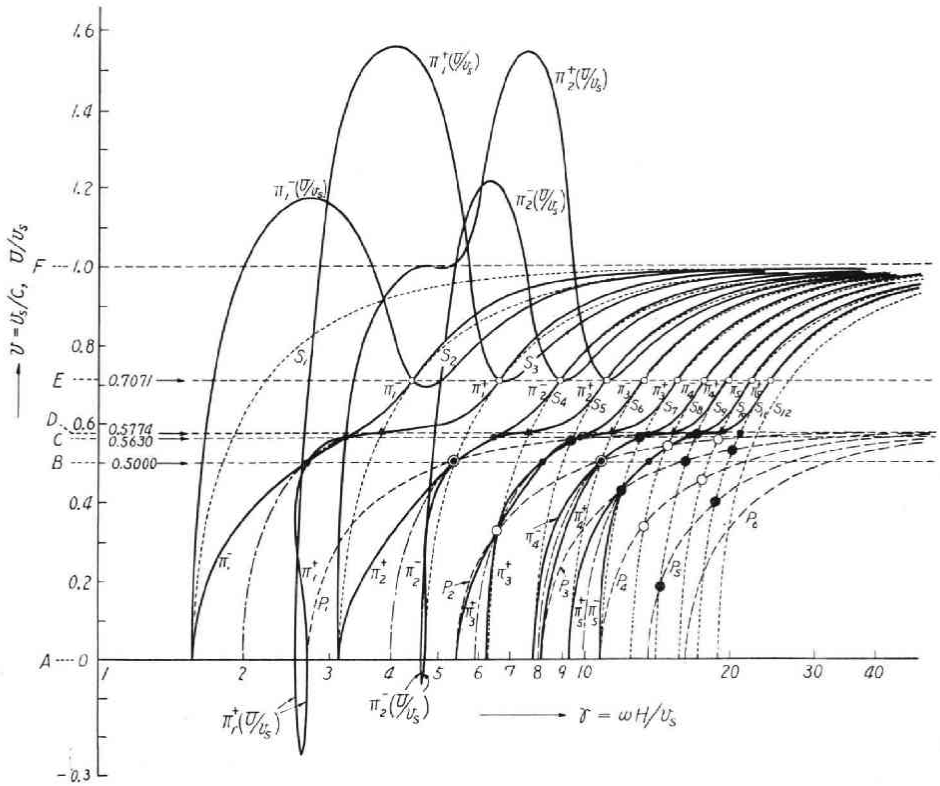

Fig. 4. Dispersion curves of an elastic plate with the Poisson ratio 1/4.
Π^+_n: symmetric mode, Π_n^-: antisymmetric mode.
P_l: $\begin{cases}\sin\alpha=0\ (l\text{: even}),\ \text{antisymmetric mode of hypothetical liquid plate } (\lambda=\lambda,\ \mu=0).\\ \cos\alpha=0\ (l\text{: odd}),\ \text{symmetric mode of}\quad''\end{cases}$
S_m: $\begin{cases}\sin\beta=0\ (m\text{: even}),\ \text{symmetric mode of hypothetical incompressible solid plate.}\\ \qquad(\lambda=\infty,\ \mu=\mu)\\ \cos\beta=0\ (m\text{: odd}),\ \text{antisymmetric mode of}\quad''\end{cases}$
●: lattice points $\cos\alpha=\cos\beta=0$.
○: lattice points $\sin\alpha=\sin\beta=0$.
◉: points of double crossing.

Since the characteristic equations imply two facts, (1) the reflection law at the surfaces, (2) the condition of constructive interference, we may infer some features of

the dispersion curves from the results above obtained. First, we expect that, at $v=0$, $1/\sqrt{2}$ and 1, the dispersion curves osculate to one of the curves (36)–(39), and that, at $v=1/2$, the curves pass through the points of intersection of certain curves of (36)–(39). Secondly, since l and m measure the wave numbers contained in the breadth of the plates, the condition $n=1/2\ (l+m)$ (n: integer) will give a rough approximation of the dispersion curves of the actual plate for the range $0<v<1/\sqrt{3}$.

Now, returning to the characteristic equations (29), we will investigate the behaviours of the dispersion curve.

5 Some Particular Properties of Dispersion Curves of Phase Velocity

In solving the characteristic equation, it is preferable to seek the value of γ for a prescribed value of v. The values of v at the particular points A,B,C,D,E and F, as shown in Figs. 2 and 3 will be used to see the general features of the dispersion curves. We are particularly interested in the real roots, and the symmetric and antisymmetric modes will be denoted, after SATÔ (1951), respectively by Π_n^+ and Π_n^-.

(A) Real Root

(i) The case $v>1$.

Because of the non-periodic nature of the characteristic equations, v is a one-valued function of γ. It is easily verified that the phase velocity of each mode approaches to the velocity of Rayleigh waves if γ is increased indefinitely. At $\gamma=0$, the symmetric mode Π_n^+ has the phase velocity of plate waves, $1.633\ v_s$ ($\lambda=\mu$), and the antisymmetric mode Π_0^- has the phase velocity $c=0$. These modes have been calculated by SATÔ rather completely.

(ii) The case $v<1$.

As seen from (32) and (33), it will be expected that the secular equations will define a many branched relations between γ and v. But, on account of their transcendental nature, the calculation of root is not straight-forward as in the case of SH-formed normal mode waves. The results of our calculation are shown in Table 1, which contains one to five modes of both types of motion, and the eigenvalues are also shown in the γ–v diagram in Fig. 4. In this figure, the particular points $A, B, \ldots . F$ are represented by the same letters to the left of the vertical axis.

To understand the general features of Fig. 4, the following considerations will be important.

(a) When v approaches to zero, $\Gamma_s=0$ and $\Gamma_a=0$ may be approximated respectively by

$$\cos\alpha = 0, \qquad \sin\beta = 0\ , \tag{40}$$

and

$$\sin\alpha = 0, \qquad \cos\beta = 0\ . \tag{41}$$

This is very natural, since $\cos\alpha=0$ and $\sin\beta=0$ represent the characteristic equations of symmetric type, respectively in the hypothetical liquid and solid plates, while $\sin\alpha=0$ or $\cos\beta=0$ corresponds to the antisymmetric modes in each plate.

When $v=0$, we have from (40),

Table of eigenvalue

v \ γ	Π_1^+	Π_2^+	Π_3^+	Π_4^+	Π_5^+
0.00	2.72070	3.14153	6.28319	8.16210	9.42478
0.02	2.71862	3.14593	6.28396		9.42770
0.04	2.71319	3.15873	6.28629	8.17929	9.43653
0.06	2.70467	3.17944	6.29026	8.20144	
0.08	2.69387	3.20739	6.29598	8.23193	9.47277
0.10	2.68161	3.24192	6.30361	8.27097	
0.12	2.66856	3.28252	6.31336	8.31837	9.53659
0.14	2.65527	3.32885	6.32549	8.37386	
0.16	2.64217	3.38073	6.34031	8.43715	9.63379
0.18	2.62959	3.43815	6.35819	8.50783	
0.20	2.61776	3.50125	6.37956	8.58538	9.77381
0.22	2.60691	3.57022	6.40495	8.66919	
0.24	2.59719	3.64539	6.43497	8.75858	9.97063
0.26	2.58878	3.72717	6.47039	8.85289	
0.28	2.58183	3.81607	6.51214	8.95163	10.24260
0.30	2.57650	3.91267	6.56139	9.05452	
0.32	2.57299	4.01761	6.61961	9.16180	10.61002
0.34	2.57154	4.13159	6.68208	9.27422	
0.36	2.57245	4.25535	6.77118	9.39329	11.08987
0.38	2.57615	4.38954	6.87031	9.52136	
0.40	2.58319	4.53483	6.99049	9.66197	11.68679
0.42	2.59441	4.69163	7.13748	9.82035	
0.44	2.61102	4.86020	7.31878	10.00448	12.38021
0.46	2.63498	5.04062	7.54357	10.22702	
0.48	2.66955	5.23347	7.82190	10.50865	13.15163
0.50	2.72070	5.44140	8.16210	10.88280	13.60350
0.52	2.80054	5.67411	8.56734	11.39580	14.18232
0.54	2.93808	5.96509	9.04467	12.08208	15.02837
0.56	3.22193	6.45992	9.71668	12.98085	16.23603
0.58	4.00775	7.99743	11.95953	15.89383	19.80501
0.60	5.21267	9.27955	13.23902	17.17462	21.10397
0.62	5.72034	9.75746	13.76648	17.77134	21.77553
0.64	6.00178	10.09862	14.18806	18.27677	22.36540
0.66	6.21786	10.40147	14.58333	18.76507	22.94681
0.68	6.41089	10.69588	14.98060	19.26529	23.54999
0.72	6.78711	11.31409	15.84105	20.36801	
0.74	6.98631	11.65714	16.32791	20.99868	25.66946
0.76	7.20068	12.03455	16.86834	21.70213	26.53592
0.78	7.43642	12.45679	17.47707	22.49736	27.51765
0.80	7.70074	12.93678	18.17277	23.40876	28.64475
0.82	8.00279	13.49164	18.98045	24.46925	29.95806
0.84	8.35507	14.14513	19.93516	25.72519	31.51523
0.86	8.77557	14.93202	21.08845	27.24489	33.40133
0.88	9.29187	15.90612	22.52036	29.13461	35.74885
0.90	9.94944	17.15675	24.36406	31.57137	38.77867
0.92	10.83069	18.84662	26.86255	34.87849	42.89442
0.94	12.10641	21.31458	30.52275	39.73093	48.93910
0.96	14.21656	25.43654	36.65651	47.87648	59.09646
0.98	18.90295	34.69004	50.47714	66.26423	82.05133
0.99	25.45635	47.72651	69.99666	92.26681	114.53700

$$\begin{cases} \gamma = \sqrt{3}\,\dfrac{l}{2}\pi\,, & l = 1, 3, 5, \ldots. \\ \gamma = \dfrac{m}{2}\pi\,, & m = 2, 4, 6, \ldots. \end{cases} \tag{42}$$

and from (41),

$$\begin{cases} \gamma = \sqrt{3}\,\dfrac{l}{2}\pi\,, & l = 2, 4, 6, \ldots. \\ \gamma = \dfrac{m}{2}\pi\,, & m = 1, 3, 5, \ldots. \end{cases} \tag{43}$$

Table of eigenvalue (continued)

v \ γ	Π_1^-	Π_2^-	Π_3^-	Π_4^-	Π_5^-
0.00	1.57080	4.71239	5.44140	7.85398	10.8828
0.02		4.71119			10.87621
0.04	1.57499	4.70805	5.46149	7.86097	10.86358
0.06		4.70312			10.85297
0.08	1.58758	4.69692	5.52033	7.88244	10.84750
0.10		4.69008			10.84814
0.12	1.60911	4.68316	5.61486	7.91961	10.85523
0.14		4.67676			10.86889
0.16	1.64032	4.67137	5.74243	7.97521	10.88922
0.18		4.66748			
0.20	1.68242	4.66551	5.90179	8.05337	10.95050
0.22		4.66588			
0.24	1.73715	4.66900	6.09295	8.16069	11.04120
0.26		4.67531			
0.28	1.80699	4.68528	6.31644	8.30749	11.16563
0.30		4.69948			
0.32	1.89544	4.71858	6.57218	8.51017	11.33181
0.34		4.74343			
0.36	2.00756	4.77517	6.85823	8.79398	11.55479
0.38		4.81527			
0.40	2.15060	4.86577	7.17125	9.19423	11.86457
0.44	2.33503	5.01088	7.51308	9.74825	12.32561
0.48	2.57501	5.25457	7.91175	10.46752	13.07095
0.50	2.72070	5.44140	8.16210	10.88280	13.60350
0.52	2.88512	5.69846	8.48976	11.34912	14.24648
0.54	3.06716	6.05214	8.97411		15.00822
0.56	3.26205	6.50911	9.73687	12.95641	16.18588
0.58	3.46089	7.00404	10.64727	14.36765	18.13854
0.60	3.65298	7.43405	11.30910	15.22051	19.14308
0.62	3.83043			15.76986	19.77359
0.64		8.05803	12.14415	16.23250	20.32109
0.66	4.13599	8.31126		16.67421	20.85595
0.68		8.55363	12.83827	17.12296	21.40766
0.70	4.39816	8.79721		17.59543	21.99454
0.72		9.05077	13.57773	18.10469	22.63165
0.74	4.65154	9.32179		18.66333	23.33410
0.76		9.61767	14.45145	19.28525	24.11904
0.78	4.92742	9.94665	14.96693	19.98722	25.00750
0.80		10.31879	15.55478	20.79077	26.02675
0.82	5.25943	10.74724	16.23605	21.72485	27.21366
0.84	5.46091	11.25012	17.04015	22.83018	28.62021
0.86	5.69798	11.85380	18.01024	24.16667	30.32311
0.88	5.98517	12.59900	19.21324	25.82749	32.44173
0.90	6.34603	13.55310	20.76041	27.96772	35.17503
0.92	6.82283	14.83865	22.85459	30.87052	38.88646
0.94	7.50236	16.71049	25.91867	35.12684	44.33501
0.96	8.60658	19.82655	31.04652	42.26650	53.48647
0.98	11.00940	26.79650	42.58360	58.37069	74.15779
0.99	14.32128	36.59143	58.86159	81.13174	103.40180

The above relations enable us to define the mode number n according to the order of increasing cut-off frequencies as shown in the table below.

mode	Π_1^+	Π_2^+	Π_3^+	Π_4^+	Π_5^+
γ	$\frac{\sqrt{3}}{2}\pi$	π	2π	$\frac{3\sqrt{3}}{2}\pi$	3π
l, m	$l=1$	$m=2$	$m=4$	$l=3$	$m=6$

(44)

mode	Π_1^-	Π_2^-	Π_3^-	Π_4^-	Π_5^-
γ	$\frac{\pi}{2}$	$\frac{3}{2}\pi$	$\sqrt{3}\pi$	$\frac{5}{2}\pi$	$2\sqrt{3}\pi$
$l,\ m$	$m=1$	$m=3$	$l=2$	$m=5$	$l=4$

(44)′

We note that, when Π_n^+ and Π_n^- are neither shear-cross modes, nor compressional-cross modes, there holds the relation

$$n=\frac{1}{2}(l+m). \tag{45}$$

Since the slopes of the curves P_l and S_m are written as

$$\left(\frac{dv}{d\gamma}\right)_{P_l}=\frac{\frac{1}{3}-v^2}{\gamma v}\ ,\quad \left(\frac{dv}{d\gamma}\right)_{S_m}=\frac{1-v^2}{\gamma v}\ , \tag{46}$$

we have, using (34) and (35),

$$\lim_{v\to 0}\left(\frac{dv}{d\gamma}\right)_{\Pi_n^{\pm}}=\lim_{v\to 0}\left(\frac{dv}{d\gamma}\right)_{P_l,\,S_m}=\infty \tag{47}$$

(b) When v approaches to E ($v=1/\sqrt{2}$), the value of γ satisfying $\Gamma_s=0$ and $\Gamma_a=0$ are given respectively by $\cos\beta=0$ and $\sin\beta=0$.

At $v=\frac{1}{\sqrt{2}}$, we have for $\Pi^+{}_n$,

$$\gamma=\sqrt{2}\,\frac{m}{2}\pi\,,\qquad m=1,3,5,\ldots. \tag{48}$$

and for $\Pi^-{}_n$,

$$\gamma=\sqrt{2}\,\frac{m}{2}\pi\,,\qquad m=2,4,6,\ldots. \tag{49}$$

The slope at $v=1/\sqrt{2}$ of both curves $\Pi_n^{\pm}$ are obtained from (35)

$$\left(\frac{dv}{d\gamma}\right)_{\Pi_n^{\pm}}=\left(\frac{dv}{d\gamma}\right)_{S_m}=\frac{1}{\sqrt{2}\gamma}\ . \tag{50}$$

As stated in the preceding section, $\cos\beta=0$ and $\sin\beta=0$ are respectively the symmetric and antisymmetric modes in an incompressible solid plate with rigid boundaries. The transition of Π_n^+ to $\cos\beta=0$ and that of Π_n^- to $\sin\beta=0$ is in accordance with the fact that the phase lag in total reflection becomes π at $E(v=1/2)$ in Fig. 2.
(c) When v approaches to D ($v=1/\sqrt{3}$), the values of γ satisfying $\Gamma_s=0$ and $\Gamma_a=0$ are respectively given by $\sin\beta=0$ and

$$v^2N\tan\beta=-a^2\gamma\,. \tag{51}$$

When $v=1/\sqrt{3}$, we have for Π_n^+,

$$\gamma=\sqrt{\frac{3}{2}}\,\frac{l}{2}\pi\,,\qquad l=2,4,6,\ldots. \tag{52}$$

and, for Π_n^-

$$\tan\left(\sqrt{\frac{2}{3}}\gamma\right)=-\frac{\sqrt{6}}{24}\gamma\ . \tag{53}$$

The roots of (53) are obtained as follows:

n	1	2	3	4	5
γ	3.4347	6.9405	10.5366	14.2063	17.9271

(54)

The slopes at D become

$$\left(\frac{dv}{d\gamma}\right)_{\Pi_n^+} = \frac{2\sqrt{3}}{51\gamma}, \tag{55}$$

$$\left(\frac{dv}{d\gamma}\right)_{\Pi_n^-} = \frac{2\sqrt{3}}{9\gamma}\left(1+\frac{\gamma^2}{108}\right). \tag{56}$$

We note that Π_n^+, and $\sin\beta=0$ intersect at D, but the behaviour of Π_n^- is somewhat irregular. This may be due to the fact that the coefficient of S-P reflection is not unity as shown in Fig. 2.

(d) When $0<v<1/\sqrt{3}$, if we put in (29), the relation

$$\frac{a^2}{v^2 M N} = 1, \tag{57}$$

then, we have

$$\tan\alpha + \tan\beta = 0. \tag{58}$$

From (58), we can write

$$\gamma\left[\sqrt{1-v^2} + \sqrt{\frac{1}{3}-v^2}\right] = n'\pi, \quad n' = 1, 2, 3, \ldots. \tag{59}$$

The equation (57), when multiplied by the equation obtained from (57) by putting the right hand side -1 instead of 1, gives the Rayleigh cubic, the roots of which are $v^2 = 1/4$, $(3\mp\sqrt{3})/4$. Of these, $1/4$ and $(3-\sqrt{3})/4$ satisfy (57), while the other root $(3+\sqrt{3})/4$ gives the velocity of Rayleigh waves. Thus, we have from (57) and (59), the points of intersection of Π_n^+ and Π_n^-,

$$\begin{cases} v = 0.5 \\ \gamma = \dfrac{\sqrt{3}}{2} n'\pi, \qquad n' = 1, 2, 3, \ldots. \end{cases} \tag{60}$$

$$\begin{cases} v = \dfrac{3-\sqrt{3}}{4} = 0.56302 \\ \gamma = \dfrac{\sqrt{3}\,[3\sqrt{1+\sqrt{3}} - \sqrt{9-5\sqrt{3}}]}{7} n'\pi = 0.95430\, n'\pi, \end{cases}$$

$$n' = 1, 2, 3, \ldots. \tag{61}$$

The points defined by (60) and (61) are shown by small black circles in Fig. 4, (55) is related to anomalous reflection, in which, for incident P and SV, only SV and P are reflected respectively. The roots $v=0.5$ and 0.56302 correspond respectively to B and C.

Since the relations $\cos\alpha=\cos\beta=0$ and $\sin\alpha=\sin\beta=0$ both satisfy (58), the curves (59) pass through the points of intersection of P_l and S_m, provided that $n' = 1/2(l+m)$, and l and m are both even or odd. Remembering (45), we see that n' is equal to n and represents the mode number.

We obtain from (34) and (35), the slopes at B

$$\left(\frac{dv}{d\gamma}\right)_{\Pi_n^{\pm}} = \frac{\sqrt{3}}{3n\pi \mp 4\sin\left(\frac{n\pi}{2}\right)}, \tag{62}$$

and at C,

$$\left(\frac{dv}{d\gamma}\right)_{\Pi_n^{\pm}} = \frac{1.78483}{n\pi \pm 1.82137 \sin(0.267949\, n\pi)}. \tag{63}$$

Numerical values of (62) and (63) are:

at B, (v=0.5),

n	1	2	3	4	5
$\left(\frac{dv}{d\gamma}\right)_{\Pi_n^+}$	0.31927	0.091888	0.053667	0.045945	0.040165
$\left(\frac{dv}{d\gamma}\right)_{\Pi_n^-}$	0.12902	0.091888	0.071353	0.045945	0.033879

(64)

at C, (v=0.5630),

n	1	2	3	4	5
$\left(\frac{dv}{d\gamma}\right)_{\Pi_n^+}$	0.39663	0.22054	0.17035	0.14679	0.12647
$\left(\frac{dv}{d\gamma}\right)_{\Pi_n^-}$	1.00094	0.39899	0.21319	0.13757	0.10315

(65)

(e) Even if (57) does not hold, con α=cos β=0 and sin α=sin β=0 always saitsfy the characteristic equations, so that the curves

$$\tan\alpha + \tan\beta = 0 \quad \text{or}$$

$$\gamma\left[\sqrt{1-v^2} + \sqrt{\frac{1}{3}-v^2}\right] = n\pi, \qquad n = 1, 2, 3, \ldots. \tag{66}$$

pass through the crossing points of P_l and S_m. In Fig. 4, (66) are drawn by chained lines. These curves may be considered to represent the first approximation for $\Pi_n^{\pm}$.

The lattice points defined by

$$\cos\alpha = 0, \qquad \cos\beta = 0, \tag{67}$$

and

$$\sin\alpha = 0, \qquad \sin\beta = 0, \tag{68}$$

are represented in Fig. 4 respectively by large black and white circles. At lattice points, the slopes of P_l and S_m are also given by (46). The slopes at the lattice points (67) of the curves $\Pi_n^{\pm}$ are obtained as

$$\left(\frac{dv}{d\gamma}\right)_{\Pi_n^+} = \frac{3(1/3-v^2)}{\gamma v(3-8v^2)}, \qquad \left(\frac{dv}{d\gamma}\right)_{\Pi_n^-} = \frac{(3-8v^2)(1-v^2)}{3\gamma v} \tag{69}$$

and at potints defined by (68), the slopes of $\Pi_n^{\pm}$ are interchanged.

It can be shown that, at the lattice points (67), we have the relation

$$\left(\frac{dv}{d\gamma}\right)_{S_m} > \left(\frac{dv}{d\gamma}\right)_{\Pi_n^-} \geqq \left(\frac{dv}{d\gamma}\right)_{\Pi_n^+} > \left(\frac{dv}{d\gamma}\right)_{P_l}, \tag{70}$$

and at the lattice points (68),

$$\left(\frac{dv}{d\gamma}\right)_{S_m} > \left(\frac{dv}{d\gamma}\right)_{\Pi_n^+} \geqq \left(\frac{dv}{d\gamma}\right)_{\Pi_n^-} > \left(\frac{dv}{d\gamma}\right)_{P_l}, \tag{71}$$

where the equal sign holds only if $v=0.5$. Thus we have seen that the slope of Π_n^+ is less than that of Π_n^- at (67), and vice versa at (68), and the slopes of both Π_n^+ and Π_n^- lie between those of S_m and P_l. These situations are illustrated in Fig. 5. a, b. (70) and (71) indicate that $\Pi_n^\pm$ oscillate about the curve (66) as shown in Fig. 5, c. As seen from (d), $\Pi_n^\pm$ intersect at the crossing point of $v=0.5$ and (66), while, if n is even, the point of intersection become lattice points. The behaviour of $\Pi_n^\pm$ resulting from the double intersection is shown in Fig. 5, c, and points of double intersection are shown by double circles in Fig. 4. Equality of the slopes of $\Pi_n^\pm$ at such particular points is indicated by the equal signs in (70) and (71).

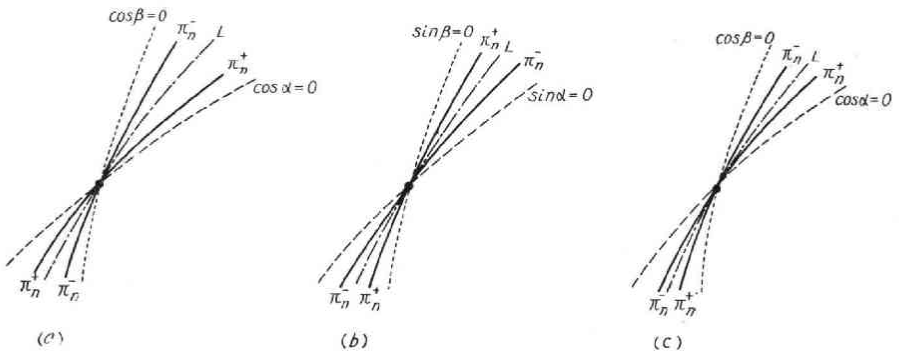

Fig. 5. Behaviours of dispersion curves at lattice points.
(a) and (b) are the cases of a single intesection of $\Pi^+{}_n$ and $\Pi^-{}_n$.
(c) is the case of a double intersection of $\Pi^+{}_n$ and $\Pi^-{}_n$.

(B) LYON (1955) has discussed the imaginary roots in his problem of the symmetric motion due to periodic forces exerted vertically at finite areas on the surface. He has shown that for a prescribed frequency, there exists only a finite number of imaginary roots. As mentioned in the first paper, imaginary roots give rise to waves of exponentially damping, so that they can be discarded in so far as the motion at large distances is concerned.

(C) Complex root

SHERWOOD (1958) has suggested the existence of infinite set of complex roots for a specified frequency. Since for any prescribed frequency there exists only a finite number of real and imaginary roots, an arbitray motion in a plate would not be accounted for without the set of infinite numbers of complex root.

In our problem, it suffices to note that complex roots are associated with standing waves. It is possible to show that if $v=a-ib$ is a root of $\Gamma_s=0$ or $\Gamma_a=0$, then $-a-ib$ becomes also a root of each equation.

Taking a pair of roots $\pm a-ib$ we can always write for the term containing x in (8)

$$e^{-ikx(a-ib)}+e^{-ikx(-a-ib)}=2e^{-bkx}\cos(akx)\,. \tag{72}$$

This shows the standing waves whose amplitude is attenuated exponentially along the plate. Thus, complex roots are of no importance for us.

6 Group Velocity

The group velocity U is formally defined by

$$U=\frac{d\omega}{d(k\sin w)}=v_s\frac{d(\gamma)}{d(\gamma v)}\,, \tag{73}$$

so that we can write

$$\frac{v_s}{U}=v+\gamma\frac{dv}{d\gamma}=v-\gamma\frac{\left(\frac{\partial\Gamma_{s,a}}{\partial\gamma}\right)}{\left(\frac{\partial\Gamma_{s,a}}{\partial v}\right)}\,. \tag{74}$$

From (34) and (74), we obtain for Π_n^+,

$$\frac{U}{v_s}=\frac{v\left[3\alpha a^2+4a\left(2v^4-4v^2+1\right)\tan\alpha-v^2N^2(8v^2-3)\,\alpha.\tan\alpha^2\right]}{\left[\alpha a^2\left(8v^4-8v^2+3\right)+4v^2a\left(2v^4-4v^2+1\right)\tan\alpha-v^2(8v^4-1)N^2\alpha\tan^2\alpha\right]}\,. \tag{75}$$

and for Π_n^-,

$$\frac{U}{v_s}=\frac{v\left[v^2\left(8v^2-3\right)N^2\alpha+4a\left(2v^4-4v^2+1\right)\tan\alpha-3\alpha a^2\tan^2\alpha\right]}{\left[v^2\left(8v^4-1\right)N^2\alpha+4v^2a\left(2v^4-4v^2+1\right)\tan\alpha-\left(8v^4-8v^2+3\right)a^2\alpha\tan^2\alpha\right]}\,. \tag{76}$$

The group velocity for some modes are shown in Fig. 4.

Some important features of the group velocity are as follows.

(a) When $v=0$, we see from (75) and (76), that $U=0$ for both $\Pi_n^{\pm}$.

(b) When $v=1$, it is easily shown that the group velocity is equal to the velocity of S for both $\Pi_n^{\pm}$.

(c) When $v=1/\sqrt{2}$, it follows that

$$\frac{U}{v_s}=\frac{1}{\sqrt{2}}=0.7071\,. \tag{77}$$

(d) It should be noticed that, at $v=0.5$, for even n, $\Pi_n^{\pm}$ have the identical group velocity $U=v_s$ at frequency $\gamma=\sqrt{3}/2n\pi$ But, for n odd, such a conspicuous nature is not found.

(e) When $v=1/\sqrt{3}$ we obtain from (55) and (74) that, for any value of n, Π_n^+ has the same group velocity

$$\frac{U}{v_s} = \frac{17\sqrt{3}}{19} = 1.5497 . \tag{78}$$

Π_n^- has not such a simple relation.

(f) In the range $0 < v < 1/\sqrt{3}$, as can be seen from the dispersion curves of phase velocity, the dispersion curves of group velocity of the same mode number oscillate about the curves

$$\begin{cases} \dfrac{U}{v_s} = \dfrac{v}{v^2 + \sqrt{1-v^2}\sqrt{1/3-v^2}} , \\ \gamma = \dfrac{n\pi}{\sqrt{1-v^2} + \sqrt{1/3-v^2}} . \end{cases} \tag{79}$$

This feature is clearly shown in the curves of $\Pi_{49}^{\pm}$ calculated by TOLSTOY and USDIN.

(g) The maximum group velocity in higher modes approaches to the velocity of P. This can be seen from Fig. 6, which schematically shows the behaviours of $\Pi_n^{\pm}$ at the lattice points with small l and large m, The maximum group velocity and the corresponding frequency can be calculated. Putting $l=1$, $m=2n-1$ in (36) and (38), we obtain

$$\gamma = \frac{\pi}{2}\sqrt{6n(n-1)} , \tag{80}$$

$$v = \sqrt{\frac{2n^2-2n-1}{6n(n-1)}} . \tag{81}$$

Substituting (80) and (81) into (69) and (74), we have

$$\left(\frac{dv}{d\gamma}\right)_{\Pi_n^+} = \frac{3}{\pi(n^2-n+4)\sqrt{2n^2-2n+1}} , \tag{82}$$

$$\frac{U}{v_s} = \frac{(n^2-n+4)\sqrt{2n^2-2n-1}\sqrt{6n(n-1)}}{(n^2-n+4)(2n^2-2n+1)+9n(n-1)} . \tag{83}$$

If we put $n=49$ in (83) we have, $U/v_s = 1.729$, so the group velocity is practically equal to the velocity of P. These values are concordant with those calculated by TOLSTOY and USDIN.

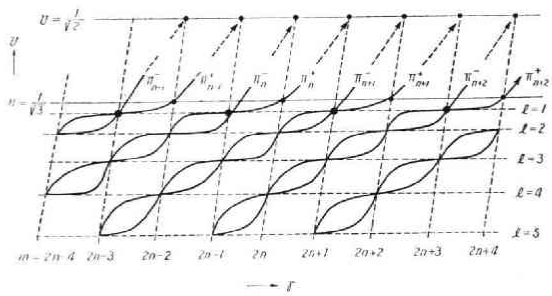

Fig. 6. Eigenvalues in higher modes.

7 A Remark on the Pahse and Group Velocities

From Fig. 4, we see that the phase velocitis for Π_1^+ and Π_2^- become the two-valued function of γ near the cut-off frequencies, and correspondingly, the group velocities

become nagative. This situation is shown more clearly in Fig. 7 for the mode Π_1^+. It is possible to verify that the inflection point C of the curve v corresponds to the point B, and the branch CA yields the negative part BDA of the curve U/v_s, while the other branch CE corresponds to the positive part BF. TOLSTOY and USDIN (1956) have found this fact. They, confining their attention to the branch CA, have supposed that the phase velocity must be negative as the group velocity is essentially to be positive. But, there seems to be no reason why the group velocity must be positive in that brach. If a source were a peculiar type such that only S wave rays with a band of incident angles represented by CB are produced, the energy would be transmitted towards the source. In a simple harmonic excitation of a point source usually assumed, we must always consider, for a prescribed frequency denoted by G, the residue contributions from the two poles corresponding to H and I. So that two group velocities denoted by D and J are to be considered. Detailed calculation shows that, in the frequency range BA, the magnitude of the positive group velocity is larger than the absolute value of the negative group velocity. Also, from the amplitude calculation which will be described in the next paper, it can be shown that the excited amplitude for the branch BF is always larger than that for the branch BDA. From these facts, it can be verified that, at large distances from the source, only diverging waves can exist, since, according to BIOT, the group velocity written formally by (73) represents the rate of energy transfer.

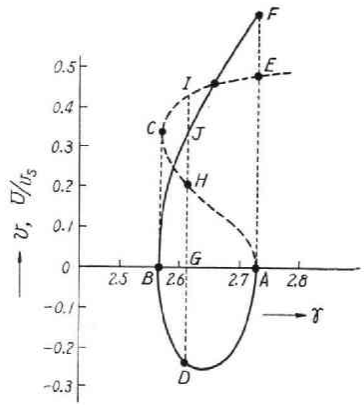

Fig. 7. Enlarged figure of the dispersion curve of Π_1^+ in which negative group velocity appears.

8 Summary

Dispersive property of an elastic plate with the Poisson ratio 1/4 is investigated by use of $\gamma-v$, $\gamma-U/v_s$ diagrams, where $\gamma=\omega H/v_s$., $v=v_s/c$ and c and U represent respectively the phase and group velocities. The lowest modes $\Pi_0^{\pm}$ are excluded in most part of the discussion.

Since characteristic equations represent the conditions of constructive interference of P and S waves which generate both P and S on reflection at the boundaries by the definite law of reflection, the reflection law is examined at first.

At particular incident angles of S represented by A,E,F, in Fig. 2, P–S, S–P transformations do not occur, and at anglescor responding to B and C in the same figure, P–S, S–P transformations are perfect. It is shown that, at E, F, A, the dispersion curves coincide with those of liquid or incompressible solid plate, and the coincidence of symmetric and antisymmetric nature of motion is also verified.

In the range $1/\sqrt{3}>v>0$, the characteristic equations are satisfied whenever $\cos\alpha$

$=\cos\beta=0$ and $\sin\alpha=\sin\beta=0$, so that the curves of $\Pi_n^{\pm}$ intersect at the lattice points defined by those relations. $\cos\alpha=0$ and $\cos\beta=0$ represent the dispersion curves respectively of the symmetric and antisymmetric modes in a liquid plate, and $\sin\alpha=0$, $\sin\beta=0$ correspond to the symmetric and antisymmetric modes in an incompressible solid plate. At lattice points $\cos\alpha=\cos\beta=0$, Π_n^{+} couples more strongly with the symmetric mode in a liquid plate than with the antisymmetric mode in a solid plate, while at lattice points $\sin\alpha=\sin\beta=0$, Π_n^{+} couples more strongly with the symmetric mode in a solid plate than with the antisymmetric mode in a liquid plate.

Besides lattice points, $\Pi_n^{\pm}$ intersect each other on the lines given by B and C. The even modes of Π_n^{+} intersect twice at lattice points on the line $v=1/2$ in Fig. 4. At the frequencies of such twice intersection, Π_n^{+} (n: even) gives always the group velocity equal to the velocity of S. At the incident angle 45° (E), whole modes give the group velocity equal to $1/\sqrt{2}v_s$. In comparatively high modes, the maximum group velocity becomes practically equal to the velocity of P. Such maximum group velocity and the corresponding frequency are given by functions of mode number.

A brief account is given on the "negative phase velocity".

References

1. AGGARWAL, R.R. (1952): Axially symmetric Vibration of a Finite Isotropic Disk, *J. Acoust. Soc. Amer.*, **24**, 463–467.
2. AGGARWAL, R.R. (1952): Axially symmetric Vibration of a Finite Isotropic Disk, *J. Acoust., Soc. Amer.*, **24**, 663–666.
3. AGGARWAL, R.R. (1953): Axially symmetric Vibration of a Finite Isotoropic Disk, *J. Acoust. Soc. Amer.*, **25**, 533.
4. AGGARWAL, R.R. and E.A.G. SHOW. (1954): Axially symmetric Vibration of a Isotropic Disk, *J. Acoust. Soc. Amer.*, **26**, 341–342.
5. BANKROFT, D. (1941): The Velocity of Longitudinal Waves in Cylindrical Bars, *Phys. Rev.*, **59**, 588–593.
6. FAY R.D. and O.V. FORTIER. (1951): Transmission of Sound through Steal Plates immersed in Water, *J. Acoust. Soc. Amer.*, **23**, 339–346.
7. FAY, R.D. (1953): Notes on the Transmission of Sound Through Plates, *J. Acoust. Soc. Amer.*, **25**, 220–223.
8. HOLDEN, A.N. (1951): Longitudinal Modes of Elastic Waves in Isotropic Cylinders and Slabs, Bell System Tech, J., **30**, 956–699.
9. HUDSON, C.E. (1943): Dispersion of Elastic Waves in Solid Circular Cylinders, *Phys. Rev.*, **63**, 46–51.
10. LAMB, H. (1917): On Waves in an Elastic Plate, *Proc. Roy. Soc.*, A, **93**, 114–128.
11. LOVE, A.E.H. (1911): "Some Problems of Geodynamics", Cambridge Univ. Press, London.
12. LYON, R.H. (1955): Response of an Elastic Plate to Localized Driving Force, *J. Acoust. Soc. Amer.*, **27**, 259-265.
13. MORSE, R.W. (1948): Dispersion of Compressional Waves in Isotropic Rods of Rectangular Cross Section, *J. Acoust. Soc. Amer.*, **20**, 833–835.
14. MINDLIN, R.D. (1951): Influence of Rotatory Inertia and Shear on Flexural Motions of Isotropic Elastic Plates, *J. Appl. Mechanics*, **18**, 31–38.
15. MINDLIN, R.D. (1951): Thickness-Shear and Flexural Vibration of Crystal Plates, *J. Appl. Physics*, **22**, 316–323.
16. RAYLEIGH, LORD : (1889): On the free Vibration of an Infinite Plate of Homogeneous Isotropic Elastic Matter, *Proc. London. Math. Soc.*, **20**, 225.

17. SATÔ, Y. (1951): Study on Surface Waves. II: Velocity of Surface Waves Propagated upon Elastic Plates, *Bull. Earthquake Res. Inst.* (Tokyo) **29**, 223–261.
18. SHERWOOD, J.W.C. (1958): Propagation in an Infinite Elastic Plate, *J. Acoust. Soc. Amer.* **30**, 979–984.
19. TAJIME, K. (1958): Transmission from Solid to Liquid Superficial Waves in a Plate. *J. Phys. Earth* **5**, 91-99.
20. TOLSTOY, I. (1954): Note on the Propagation of Normal Modes in Inhomogeneous Media, *J. Acoust. Soc. Amer.*, **27**, 274–277.
21. TOLSTOY, I. (1955): Dispersion and Simple Harmonic Point Source in Wave Duct, *J. Acous. Soc. Amer.*, **27**, 897–907.
22. TOLSTOY, I. (1956): Resonant Frequencies and High Modes in Layered Wave Guides, *J. Acoust. Soc. Amer.*, **28**, 1182–1192.
23. TOLSTOY, I. (1957). Wave Propagation in Elastic Plates: Low and High Mode Dispersion, *J. Acoust. Soc. Amer.*, **29**, 37–42.
24. TOLSTOY, I. (1958): Shallow Water Test of the Theory of Layerd Wave guides, **30**, *J. Acoust. Soc. Amer.* **30**, 348–361.